

Scientific paper

# New Insights into CAZ-AVI's Pharmacological Mechanisms: Network Pharmacology and Molecular Docking Reveal Molecular Targets in Pneumonia Treatment

Kun Zhang\*, Yu-Qian Cheng, Cun-Jin Wu\*

Department of Infectious Diseases, The Second Hospital of Tianjin Medical University, Tianjin 300211, People's Republic of China

\* Corresponding author: E-mail: zhangkunlz1103@163.com; wucunjin.99@163.com

Received: 08-27-2025

#### **Abstract**

Ceftazidime-Avibactam (CAZ-AVI) has demonstrated good efficacy in treating pneumonia. Currently, research on CAZ-AVI is primarily focused on its direct antibacterial effects, while exploration of its potential host targets remains relatively limited. In light of this, our study innovatively employs a research strategy that integrates network pharmacology and computer-aided drug design to systematically explore the potential host targets of CAZ-AVI. We identified 141 intersecting targets in CAZ-AVI-treated pneumonia, with key targets including Epidermal Growth Factor Receptor (EGFR), Src Proto-Oncogene (SRC), Signal Transducer and Activator of Transcription 3 (STAT3), Heat Shock Protein 90 Alpha Family Class A Member 1 (HSP90AA1), Caspase 3 (CASP3) and Nuclear Factor Kappa B Subunit 1 (NFKB1). By inhibiting or activating these target proteins, CAZ-AVI plays a significant regulatory role in cell proliferation, apoptosis, signal transduction, and immune responses. Our experimental results further confirmed that the compound possesses activities in inhibiting cell proliferation and promoting apoptosis. CAZ-AVI can correct cellular dysfunction and optimize immune responses, thereby providing new strategies and insights for the treatment of pneumonia.

Keywords: Ceftazidime-Avibactam, Pneumonia, Network Pharmacology, Molecular docking.

#### 1. Introduction

Pneumonia is a disease with a high incidence rate worldwide, especially hospital-acquired pneumonia (HAP) and ventilator-associated pneumonia (VAP). 1-2 The prevalence of multidrug-resistant (MDR) bacteria has further complicated treatment, leading to increasing difficulty in managing these conditions year by year.3-4 Ceftazidime-Avibactam (CAZ-AVI) is an antibacterial combination composed of ceftazidime, a third-generation cephalosporin, and avibactam, a novel non- $\beta$ -lactam  $\beta$ -lactamase inhibitor.<sup>5-7</sup> It has been approved for the treatment of complex infections, including HAP and VAP. CAZ-AVI enhances the antibacterial activity of ceftazidime by inhibiting bacterial  $\beta$ -lactamases, thereby effectively combating a wide range of drug-resistant bacteria, 8-10 such as KPC-producing Klebsiella pneumoniae (KPC-Kp) and carbapenem-resistant Enterobacteriaceae (CRE).

Currently, research on CAZ-AVI is primarily focused on its direct antibacterial effects, 11-13 while exploration of its potential host targets remains relatively limited. However, recent studies have indicated that this drug may indirectly

influence the outcomes of infectious diseases through multiple pathways, such as modulating the host immune response, regulating inflammatory signaling pathways, and promoting tissue repair mechanisms. 14–16 This finding offers a new perspective for a deeper understanding of the pharmacological mechanisms of CAZ-AVI. Elucidating these potential mechanisms of action will not only help optimize clinical strategies for the use of CAZ-AVI but also provide a theoretical basis for the development of new therapeutic targets against drug-resistant bacterial infections.

In this study, we innovatively employed a research strategy that integrates network pharmacology and computer-aided drug design to systematically explore the potential host targets of CAZ-AVI. By leveraging cutting-edge technologies such as bioinformatics, molecular docking, and network analysis, we constructed a multidimensional interaction network of "drug-target-pathway-disease". We hope that this approach will not only expand our understanding of the mechanisms of action of CAZ-AVI but also provide valuable insights for the development of novel therapeutic strategies against drug-resistant bacterial infections.

# 2. Experimental

### 2. 1. Acquisition of Active Ingredient Targets

The SMILES files of the active ingredients ceftazidime and avibactam were obtained from the PubChem database. These SMILES files were then imported into the Swiss Target Prediction database<sup>17</sup> (http://www.swisstargetprediction.ch/) and SuperPred database<sup>18</sup> (https://prediction.charite.de/subpages/target\_prediction.php) for target prediction.

### 2. 2. Pneumonia-Related Target Collection

Initially, known therapeutic targets for pneumonia were retrieved from the GeneCards databases<sup>19</sup> (https://www.genecards.org/) and DisGeNET databases<sup>20</sup> (http://www.disgenet.org/) using the keyword "pneumonia". Subsequently, the gene names of these identified therapeutic targets were input into the UniProt database<sup>21</sup> (https://www.uniprot.org) to locate corresponding proteins in "Homo sapien". Thereafter, the 3D structures of these proteins were downloaded from the RCSB PDB database<sup>22</sup> (http://rcsb.org/). By leveraging these four databases, we obtained potential human pneumonia-related target proteins.

# 2. 3. Screening for Pneumonia and Drug-Disease Intersection Targets

The ceftazidime and avibactam targets set and the pneumonia-related gene set was imported into a Venn Diagram (https://bioinformatics.psb.ugent.be/webtools/Venn/) for further analysis. The main potential therapeutic targets were identified based on the intersecting gene targets.

# 2. 4. Construction of Drug-Target Disease Network

A protein-protein interaction (PPI) network was generated to identify interacting proteins. The STRING database version 12.0 (http://string-db.org) was used to construct a PPI network for the antipneumonic effect of CAZ-AVI, with the species restricted to "Homo sapiens" and an interaction score greater than 0.4. The PPI network was then automatically transferred to Cytoscape 3.10.2 using the "Send Network to Cytoscape" option connected to the String App. Cytoscape plug-in Cytohubba was used to analyze topological parameters and select key treatment targets.

# 2. 5. Gene Ontology (GO) and Kyoto Encyclopedia of Genes and Genomes (KEGG) Pathway Enrichment Analyses

To further investigate the molecular mechanism of CAZ-AVI against pneumonia, GO and KEGG pathway

analyses were performed using the David database (https://david.ncifcrf.gov/home.jsp). The GO enrichment analysis encompasses three main categories: biological process (BP), molecular function (MF), and cellular component (CC). KEGG pathway analysis was conducted to enhance understanding of the interactions and functions of these targets. The top 10 BP, CC, MF, and 20 KEGG pathways were selected with a P-value ≤ 0.05.

#### 2. 6. Molecular Docking

Molecular docking of compounds into the six target proteins was performed using AutoDock 4.2.6 with the corresponding protocol, and interaction force diagrams are plotted using PyMOL software<sup>23–24</sup>. The 3D structures of protein in the docking study were downloaded from Protein Data Bank. All bound waters and ligands were eliminated from the protein, and the polar hydrogen was added to the proteins. In our docking simulations, we defined the active site based on the location of the native co-crystallized ligand in each protein structure. Prior to docking, the original co-crystallized small molecule ligand was removed from the binding site. The ligand-binding sites of all these proteins contain a substantial number of hydrophobic amino acid residues, forming a predominantly hydrophobic environment. This serves as the foundation for high-affinity binding of small molecule ligands through hydrophobic effects and van der Waals forces. Furthermore, a few key residues critical for binding or catalysis are present in each active site; these residues represent central anchor points for drug molecule design.

# 2. 7. Experimental Protocol for Investigating the Effects of CAZ-AVI on Host Cells

To investigate the effects of CAZ-AVI on host cells, the following experimental protocol was designed. First, A549 cells were seeded in 96-well plates at a density of 5,000 cells per well in 100  $\mu$ L of complete DMEM medium and incubated at 37 °C with 5% CO<sub>2</sub> until they reached 80% confluence, which typically took about 24 hours. Next, CAZ-AVI was prepared at various concentrations (5, 10, 20, and 50 mg/L), and the cells were treated with these CAZ-AVI concentrations for 24, 48, and 72 hours. A control group treated with vehicle only was also included. To assess cell viability, 20 µL of MTT solution (5 mg/mL) was added to each well and incubated for 4 hours at 37 °C. After incubation, the medium was removed, and 150 µL of DMSO was added to dissolve the formazan crystals. Finally, the absorbance was measured at 490 nm using a microplate reader.

We employed CAZ-AVI at the conventional concentration of 20 mg/L to further investigate its ability to induce apoptosis. The apoptosis was assessed using flow cytometry after treatment for 24, 48, and 72 hours. The cells were stained with Annexin V-FITC and propidium iodide

(PI) staining buffer, suspended at a concentration of  $1\times10^6$  cells/mL in  $10^5~\mu$ L of staining solution. The cells were then incubated in the dark at room temperature for 10–20 minutes before immediate detection by flow cytometry.

#### 3. Results and Discussion

#### 3. 1. Acquisition of CAZ-AVI Target

The target points of ceftazidime and avibactam were obtained by the TCMSP Database and predicted by the Swiss-Target-Prediction and SuperPred database, respectively. After merging target data and deleting duplicate values, 106 cefazidime and 149 avibactam targets were saved and standardized by the UniProt database. The target information is shown in Table S1. These collected targets may be those that could have an impact on the human body under the influence of the drug CAZ - AVI.

#### 3. 2. Target Acquisition of Pneumonia Disease

After searching for genes related to pneumonia in the GeneCards and DisGeNET databases, merging the two databases, and removing duplicate data, the targets were screened using the median Score value when the number of targets was excessive, yielding a total of 4,237 targets, shown in Table S2. The Venn diagram was plotted through the online-accessible tools, after which 141 intersection targets were obtained (Figure 1), and the detailed information of these intersection targets are listed in Table S3. The 141 collected targets may be the relevant targets that could have an impact on the human body during the treatment of pneumonia with the drug CAZ - AVI.

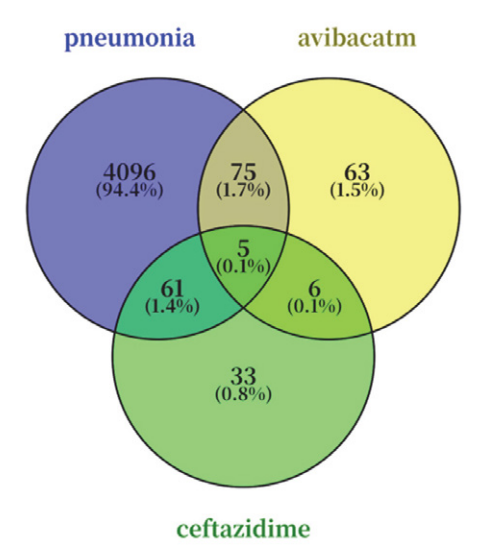


**Figure 1.** Venn diagram was used to show all candidate, interaction targets of CAZ-AVI and pneumonia.

Meanwhile, the STRING database was used to analyze the 141 targets with function-related PPI data; the

pharmacological targets of CAZ-AVI-treated pneumonia and the function-related PPI network were constructed as shown in Figure 2. In the PPI network diagram, nodes represent proteins, and edges represent interactions between proteins. To more clearly analyze the importance of each node protein within the entire network, we have conducted a visualization analysis with the aid of Cytoscape software.

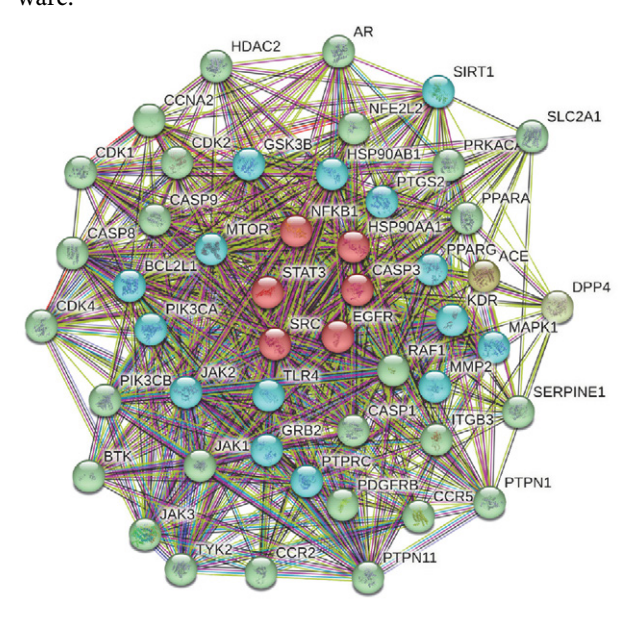


**Figure 2.** A total of 141 interaction targets in CAZ-AVI-treated pneumonia were used for PPI network visualization (Only the top targets are depicted).

# 3. 3. PPI Network Topology Parameters and Core Targets

The mapped proteins were imported into the Cytoscape software to calculate the topological parameters of the interaction network of CAZ-AVI-treated pneumonia targets and function-related proteins. To further optimize the display effect of the network diagram, we have chosen a circular layout to arrange the nodes and used the size of the nodes as well as the depth of their colors to make distinctions. Through this design, we are able to more clearly and intuitively present the interactions between the target proteins. As shown in Figure 3, we have successfully identified six core target proteins, namely Epidermal Growth Factor Receptor (EGFR), Proto-oncogene Tyrosine Protein Kinase SRC (SRC), Signal Transducer and Activator of Transcription 3 (STAT3), Heat Shock Protein 90 Alpha Subunit 1 (HSP90AA1), Caspase 3 (CASP3), and Nuclear Factor Kappa B Subunit 1 (NFKB1). (Figure 3). While CAZ - AVI is treating pneumonia, it may influence cell proliferation, survival, apoptosis, and immune responses by modulating the activity of these six core target proteins.

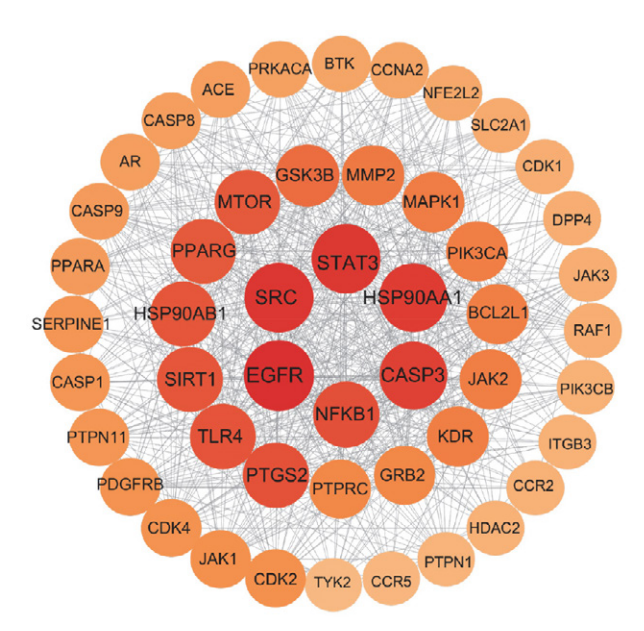


**Figure 3.** Top 6 key gene targets of bioactive ingredients ranked by degree method in Cytoscape.

# 3. 4. Enrichment Analysis of Target Function and Pathway

To understand the biological process of CAZ-AVI regulating pneumonia diseases, an enrichment analysis of GO and KEGG pathways was carried out. GO and KEGG analyses were performed on 141 targets using the David database. The top 10 enriched GO terms (BP, MF, and CC) were identified and are shown in Figure 4. The biological processes that CAZ-AVI mainly participates in include signal transduction, proteolysis, inflammatory response, response to xenobiotic stimulus, positive regulation of cell

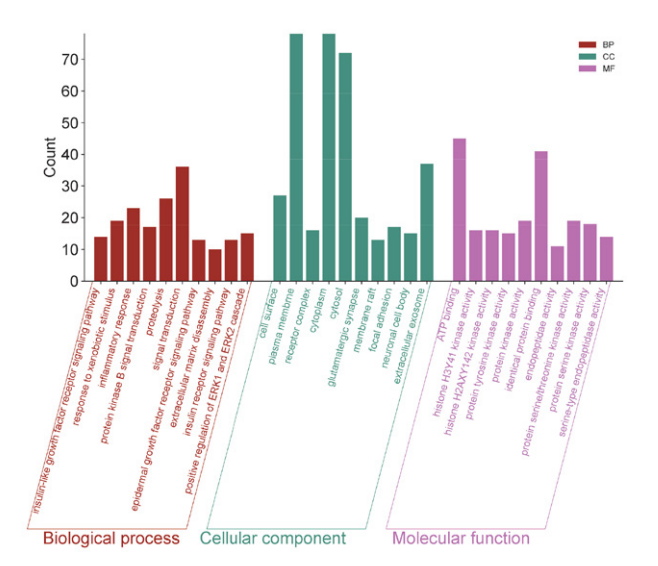
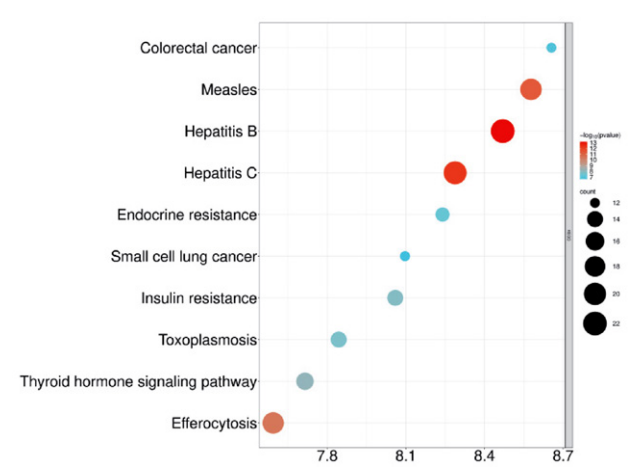


**Figure 4.** Enrichment analysis of CAZ-AVI major targets. Green is biological process enrichment analysis, orange is cellular component enrichment analysis, purple is molecular function enrichment analysis.

population proliferation, et al. The functional proteins with related targets that regulate diseases were mainly enriched in the plasma membrane, cytoplasm, cytosol, extracellular exosome, et al. The main molecular function of functional proteins that ATP binding, identical protein binding, protein kinase activity, protein serine/threonine kinase activity, etc.

The top 10 KEGG pathways are depicted in Figure 5 in a dot plot and the top 20 KEEG pathways, relevant targets in the signaling pathway of pneumonia is illustrated in Table 1. The pathways involved mainly include Hepatitis B and C, Measles, Efferocytosis, Thyroid hormone signaling pathway, Insulin resistance, Toxoplasmosis, etc. The molecular functions and biological processes associated with the target proteins of CAZ-AVI are closely related to the occurrence and progression of pneumonia, indicating that CAZ-AVI can treat pneumonia through multiple targets and biological pathways.



 $\label{eq:Figure 5.} \textbf{Figure 5.} \ \textbf{KEGG} \ \textbf{pathway} \ \textbf{enrichment} \ \textbf{bubble} \ \textbf{diagram} \ \textbf{of} \ \textbf{CAZ-AVI} \ \textbf{targets}.$ 

#### 3. 5. Molecular Docking

Molecular docking was performed to validate the interaction of the six main target proteins, namely EGFR (PDB ID: 1M17), CASP3 (PDB ID: 1GFW) and SRC (PDB ID:1A08), STAT3 (PDB ID: 6NJS), HSP90 $\alpha$  (PDB ID: 6GQR) and NF $\kappa$ B1 (PDB ID: 3RZF) with two compounds, ceftazidime and avibactam. The -CDOCKER INTERAC-TION ENERGY (kcal/mol) results of the compound with six target proteins are shown in Table 2. From the results, we can see that the binding energy values of cefotaxime with each target protein are very small. Except for STAT3, these values are much lower than those of Avibactam. This indicates that cefotaxime has a higher affinity for these target proteins and can bind to them more effectively, thereby exerting its antibacterial action. The low docking scores suggest that the scoring function values are merely a reference and do not directly equate to weak binding affinity between the compound and the protein. Therefore, we will

**Table 1.** Enrichment results from target pathways of CAZ-AVI in regulating pneumonia disease.

Pathway ID and Pathway	pvalue	count	Genes	
hsa05161: Hepatitis B	7.01.10 <sup>-14</sup>	22	MAP2K2, CHUK, <b>SRC</b> , <b>STAT3</b> , PIK3CD, TYK2, PIK3CB, <b>NF</b> κ <b>B1</b> , CASP9, CCNA2, CASP8, PIK3CA, <b>CASP3</b> , CDK2, PTK2B, MAPK1, GRB2, JAK2, RAF1, JAK3, TLR4, JAK1	
hsa05160: Hepatitis C	4.62·10 <sup>-13</sup>	21	GSK3B, MAP2K2, CHUK, <b>STAT3</b> , PIK3CD, NR1H3, TYK2, PIK3CB, <b>EGFR</b> , <b>NF</b> κ <b>B1</b> , CASP9, CASP8, PIK3CA, CDK4, <b>CASP3</b> , CDK2, MAPK1, GRB2, RAF1, PPARA, JAK1	
hsa05162: Measles	4.52·10 <sup>-12</sup>	19	GSK3B, CHUK, CSNK2A2, <b>STAT3</b> , PIK3CD, TYK2, PIK3CB, <b>NF</b> κ <b>B</b> 1 CASP9, CASP8, PIK3CA, CDK4, <b>CASP3</b> , CSNK2B, CDK2, JAK3, TLR4, JAK1, BCL2L1	
hsa04148: Efferocytosis	3.66·10 <sup>-11</sup>	19	P2RY12, CPT1A, MAP2K2, ITGB3, SLC2A1, ADAM10, NR1H3, PTPN11, PTGS2, SIRT1, AXL, <b>CASP3</b> , ALOX5, CASP1, MAPK1, ITGAV, PPARG, JAK2, PPARD	
hsa04919: Thyroid hormone signaling pathway	6.23·10 <sup>-9</sup>	15	GSK3B, HDAC2, MAP2K2, <b>SRC</b> , ITGB3, SLC2A1, PIK3CD, PIK3CB, MTOR, CASP9, PIK3CA, MAPK1, ITGAV, RAF1, PRKACA	
hsa04931: Insulin resistance	1.39·10 <sup>-8</sup>	14	PTPN1, GSK3B, PRKAA1, CPT1A, <b>STAT3</b> , SLC2A1, PIK3CD, NR1H3, PTPN11, PIK3CB, MTOR, <b>NFκB1</b> , PIK3CA, PPARA	
hsa05145: Toxoplasmosis	1.95·10 <sup>-8</sup>	14	CHUK, <b>STAT3</b> , TYK2, <b>NFκB1</b> , CASP9, CASP8, <b>CASP3</b> , ALOX5, MAPK1, JAK2, CCR5, TLR4, JAK1, BCL2L1	
hsa01522: Endocrine resistance	4.30·10 <sup>-8</sup>	13	MAP2K2, <b>SRC</b> , MMP2, PIK3CD, PIK3CB, <b>EGFR</b> , MTOR, PIK3CA, CDK4, MAPK1, GRB2, RAF1, PRKACA	
hsa05210: Colorectal cancer	1.04·10 <sup>-7</sup>	12	CASP9, GSK3B, MAP2K2, PIK3CA, <b>CASP3</b> , MAPK1, PIK3CD, GRB2, PIK3CB, RAF1, <b>EGFR</b> , MTOR	
hsa05222: Small cell lung cancer	2.08·10 <sup>-7</sup>	12	CASP9, PIK3CA, CHUK, CDK4, <b>CASP3</b> , CDK2, PIK3CD, ITGAV, PIK3CB, PTGS2, <b>NF</b> $\kappa$ <b>B1</b> , BCL2L1	
hsa05214: Glioma	2.76·10 <sup>-7</sup>	11	PDGFRB, MAP2K2, PIK3CA, CDK4, MAPK1, PIK3CD, GRB2, PIK3CB, RAF1, <b>EGFR</b> , MTOR	
hsa04012: ErbB signaling pathway	8.96·10 <sup>-7</sup>	11	GSK3B, MAP2K2, PIK3CA, <b>SRC</b> , MAPK1, PIK3CD, GRB2, PIK3CB, RAF1, <b>EGFR</b> , MTOR	
hsa04920: Adipocytokine signaling pathway	1.36·10 <sup>-6</sup>	10	PRKAA1, CPT1A, CHUK, <b>STAT3</b> , SLC2A1, PTPN11, JAK2, PPARA, <b>NF</b> κ <b>B1</b> , MTOR	
hsa04664: Fc epsilon RI signaling pathway	1.18·10 <sup>-5</sup>	9	MAP2K2, PIK3CA, ALOX5, BTK, MAPK1, PIK3CD, GRB2, PIK3CB, RAF1	
hsa05211: Renal cell carcinoma	1.32·10 <sup>-5</sup>	9	MAP2K2, PIK3CA, SLC2A1, MAPK1, PIK3CD, GRB2, PTPN11, PIK3CB, RAF1	
hsa05218: Melanoma	1.80·10 <sup>-5</sup>	9	PDGFRB, MAP2K2, PIK3CA, CDK4, MAPK1, PIK3CD, PIK3CB,	
vhsa04213: Longevity regulating pathway – multiple species	$5.05 \cdot 10^{-5}$	8	RAF1, <b>EGFR</b> PRKAA1, HDAC2, PIK3CA, PIK3CD, PIK3CB, PRKACA, SIRT1, MTOR	
vhsa04930: Type II diabetes mellitu	s 8.84·10 <sup>-5</sup>	7	PIK3CA, CACNA1B, MAPK1, PIK3CD, PIK3CB, GCK, MTOR	
hsa04960: Aldosterone-regulated sodium reabsorption	$2.91 \cdot 10^{-3}$	5	PIK3CA, MAPK1, PIK3CD, PIK3CB, NR3C2	
hsa04981: Folate transport and metabolism	1.26·10 <sup>-2</sup>	4	DHFR, SLC46A1, FOLH1, TYMS	

conduct a more detailed analysis of the interactions between the compound and the key amino acid residues in the protein's active site. To better illustrate the key amino acid residues in the protein active cavity sites of the two compounds, we present a schematic diagram of the interaction forces between

Table 2. The -CDOCKER\_INTERACTION\_ENERGY (kcal/mol) obtained by the CDOCKER protocol.

Compounds	-	CDOCKER_INTERACTION_ENERGY (kcal/mol)							
_	EGFR	CASP3	SRC	STAT3	HSP90α	NFkB1			
Ceftazidime	54.9157	54.8521	47.5104	35.2772	51.839	62.3653			
Avibactam	26.8875	29.769	22.8155	20.4921	29.0647	30.9758			

the small molecule ligands of the six protein cocrystals and the relevant amino acid residues in their cavity sites, as shown in Figure 6.

The Figure 6 presents six protein structures (EGFR, CASP3, SRC, STAT3, HSP90 $\alpha$ , NF $\alpha$ B1), each shows small molecule ligands bound to active sites with key amino acids. In EGFR, the ligand forms a conventional hydrogen bond with MET A:769 and exhibits pi-alkyl interactions with LYS A:721, LEU A:820, ALA A:719, and LEU A:694, along with carbon hydrogen bonds with GLN A:767 and PRO A:770. In CASP3, the ligand engages in conventional hydrogen bonds with GLY A:122, CYS A:163, and ARG B:207, pi-pi T-shaped interactions with TYR B:204 and PHE B:256, pi-alkyl interactions with MET A:61 and HIS A:121, and a pi-cation interaction with ARG B:207. In SRC, the ligand forms conventional hydrogen bonds with HIS A:204, ARG A:158, THR A:182, and GLU A:181, and various conjugation interactions with LEU A:204, LYS

A:206, CYS A:188, and ARG A:178. In STAT3, the ligand forms conventional hydrogen bonds with GLN A:644, SER A:636, GLU A:638, TYR A:657, SER A:611, and SER A:613, and interacts through conjugation interactions with PRO A:639 and VAL A:637. In HSP90 $\alpha$ , the ligand forms conventional hydrogen bonds with ASN A:106, PHE A:138, and ASP A:93, pi-alkyl interactions with ALA A:55, and pi-sigma interactions with MET A:98. In NF $\kappa$ B1, the ligand forms conventional hydrogen bonds with LEU A:21, ASP A:103, and LYS A:106, and exhibits conjugation interactions with VAL A:29, VAL A:152, MET A:96, ILE A:165, and CYS A:99. These interactions collectively underscore the diverse binding forces that stabilize the ligand within the active sites of these proteins.

Avibactam also exhibits a certain degree of affinity for these six target proteins, although its affinity is relatively weaker compared to ceftazidime. To delve deeper into the reasons behind this phenomenon, we conducted a de-

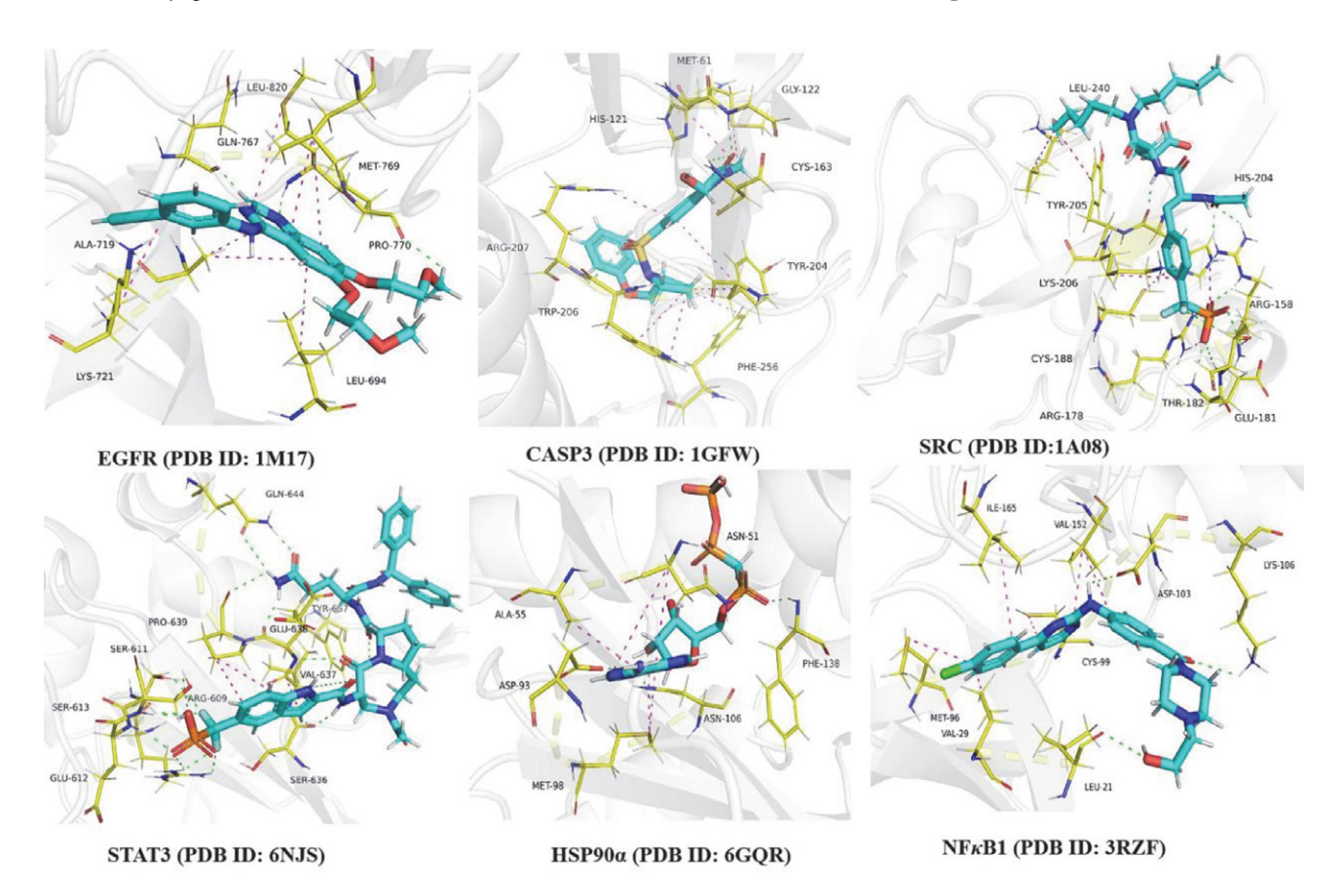


Figure 6. Schematic of interaction forces between ligands in six protein cocrystals and residues in active sites.

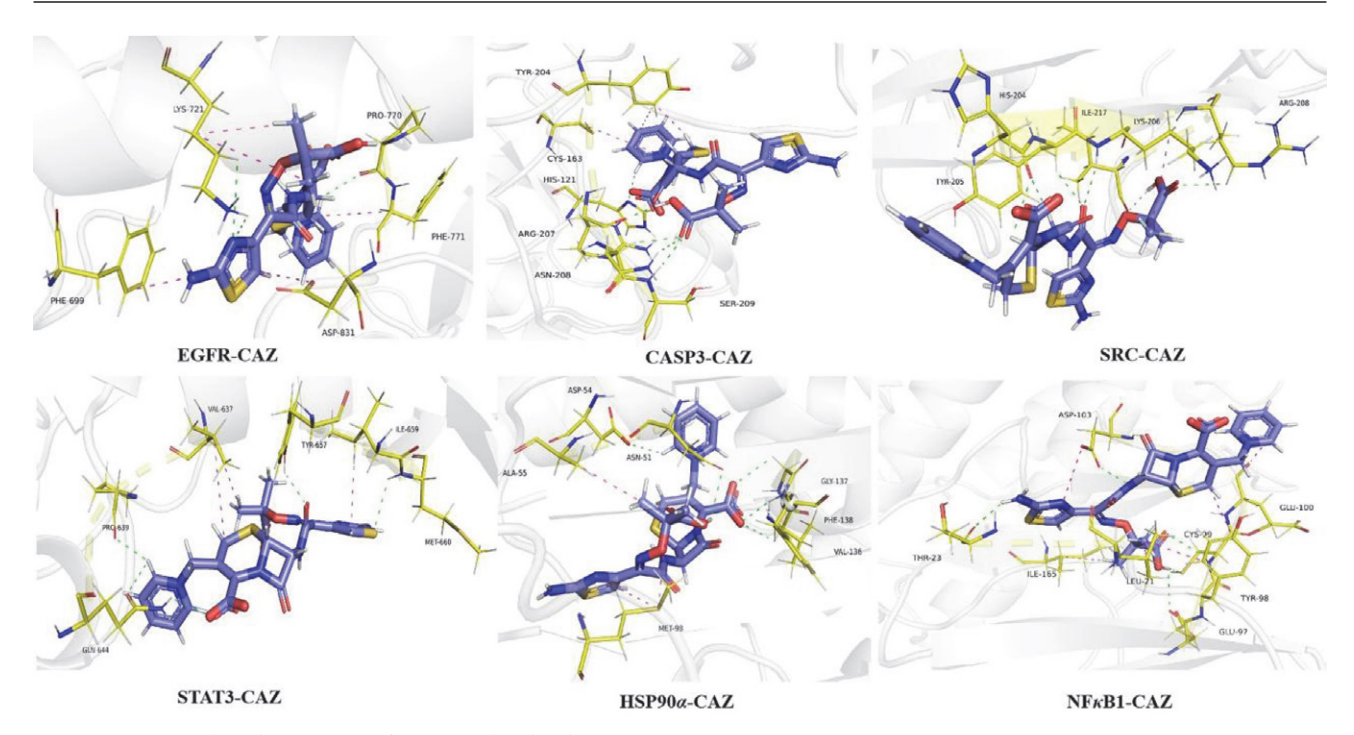


Figure 7. Protein-ligand interactions of CAZ complexed with six core targets.

tailed analysis of the three-dimensional (3D) structural diagrams of the binding sites of these two compounds with the six target proteins, as shown in Figure 7–8.

From Figures 7, we can clearly see that CAZ is capable of forming a variety of interaction forces with the target proteins, including conventional hydrogen bonds, various

conjugation interactions and so on. Compared to the original ligands of these proteins, CAZ shares many common amino acid residues at the active site. In EGFR, CAZ forms hydrogen bonds with LYS A:721, similar to the original ligand, and also with PRO A:770, stabilizing its binding to EGFR. In CASP3, CAZ interacts with HIS A:121, CYS

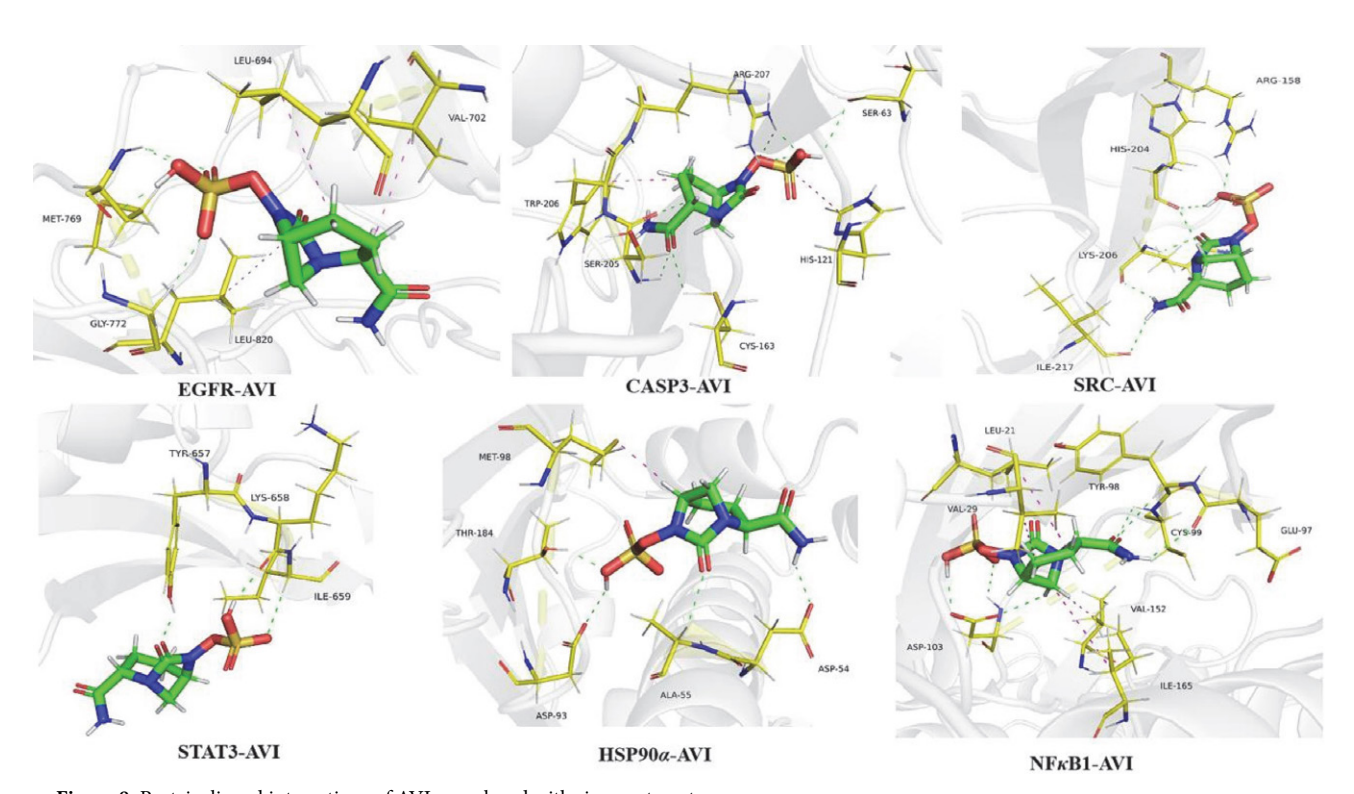


Figure 8. Protein-ligand interactions of AVI complexed with six core targets.

A:163, TYR A:204, ARG A:207, and ASN A:208, mirroring the original ligand's binding mode and explaining its strong interaction with the protein. In SRC, CAZ forms hydrogen bonds with HIS A:204, TYR A:205, and LYS A:206, mostly aligning with the original ligand's key residues. In STAT3, CAZ binds to VAL 637, PRO 639, GLN 644, and TYR 657, forming hydrogen bonds with all except TYR 657, enhancing its stability at the protein active site. In HSP90α, CAZ interacts with ASN A:51, ALA A:55, MET A:98, and PHE A:138, and additionally forms hydrogen bonds with VAL A:136 and GLY A:137, further strengthening its binding. In NFκB1, CAZ forms hydrogen bonds with LEU 21, CYS 99, ASP 103, ILE 165, THR 23, GLU 97, and ASP 103, except ILE-165 and GLU-97, stabilizing its binding to the protein. The comparative analysis shows that CAZ exhibits comparable or even stronger interaction patterns with multiple proteins than the original ligands, particularly in CASP3, HSP90α, and NF $\kappa$ B1, where its binding pattern closely matches the original ligands. This demonstrates CAZ's strong binding stability and pharmaceutical potential, indicating it holds great promise for drug development.

The Figure 8 shows that compound AVI forms multiple interactions with the six target proteins, especially strong ones like hydrogen bonds. Despite low docking scores, AVI binds effectively to the proteins' active sites. Thus, scoring functions should be used cautiously. In EGFR interactions, compound AVI forms hydrogen bonds with key amino acids MET A:769 and GLY A:772. In CASP3, it bonds with SER A:63, SER A:205, CYS A:163,

and ARG A:207. In SRC, hydrogen bonds are formed with ARG A:158, HIS A:204, LYS A:206, and ILE A:217, with most key residues matching the original ligand. In STAT3, interactions are with TYR A: 657, LYS A: 658, and ILE A: 659. In HSP90 $\alpha$ , bonds form with ASP A: 54, ALA A: 55, ASP A: 93, and THR A: 184. In NF $\kappa$ B1, interactions occur with VAL A: 29, GLU A: 97, TYR A: 98, CYS A: 99, ASP A: 103, and VAL A: 152. Besides hydrogen bonds, AVI also engages in various conjugation interactions with other amino acid residues in the protein active site, further stabilizing its binding to the protein. Interaction analysis shows that compound AVI forms hydrogen bonds with key amino acid residues in all six target proteins, demonstrating its strong binding affinity and stability. The key residues involved in these interactions mostly align with those of the original ligands, particularly in CASP3, HSP90α, and NFκB1, suggesting AVI's promising drug potential and ability to effectively engage with the proteins' active sites.

To further illustrate that the two compounds bind to the same active center of the target protein, we performed a 3D overlay of both drugs bound to the target for direct comparison, as shown in Figure 9.

Although AVI and CAZ have significantly different chemical structures, their interaction patterns with the target proteins are similar. This may explain why both compounds can act on the six target proteins. Analysis shows that both compounds interact with key amino acids HIS A:121, CYS A:163, and ARG A:207 in CASP3. This further indicates that their similar interaction patterns with these residues may be why they can act on the six

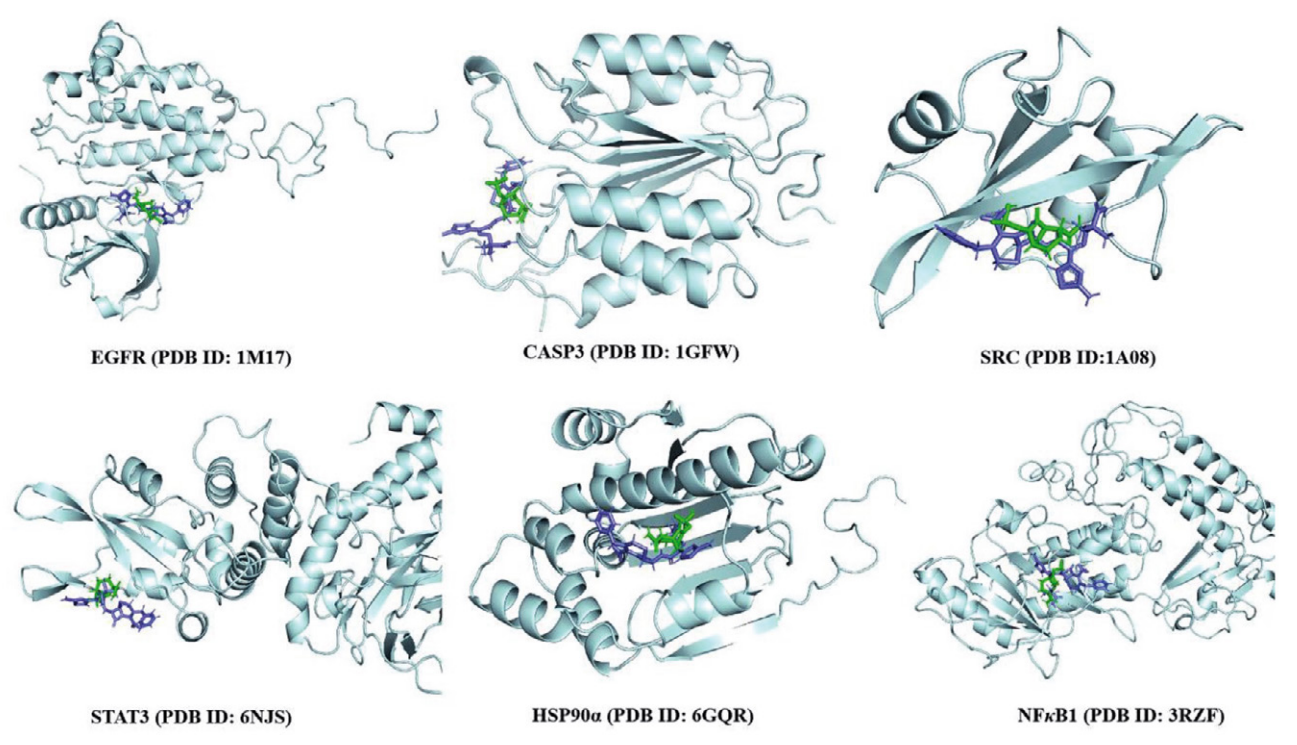


Figure 9. 3D overlay of CAZ and AVI docked to the same target.

target proteins. In SRC, both compounds interact with HIS A: 204, LYS A: 206, and ILE A: 217. In STAT3, they interact with TYR A: 657 and ILE A: 659. In HSP90 $\alpha$ , interactions are with ASP A: 54, ALA A: 55, and MET A: 98. In NF $\kappa$ B1, they interact with LEU A: 21, GLU A: 97, TYR A: 98, CYS A: 99, ASP A: 103, and ILE A: 165. These findings further indicate that the two compounds have similar interaction patterns with the target proteins.

#### 3. 6. Effects of CAZ-AVI on Host Cells

To further verify that CAZ-AVI may influence cell proliferation, survival and apoptosis, we conducted *in vit-ro* cell proliferation inhibition experiments to observe the changes in cells. As shown in the results (Figure 10), treatment with different concentrations of the drug all led to a certain degree of inhibition of cell proliferation, with the most pronounced effect observed after 24 hours of treatment. After 72 hours of treatment with low concentrations of the drug, the impact on cell proliferation was minimal. However, cells treated with high concentrations of the drug still exhibited some inhibitory effects after 48 and 72 hours. This indicates that the CAZ-AVI has a certain inhibitory effect on cell proliferation.

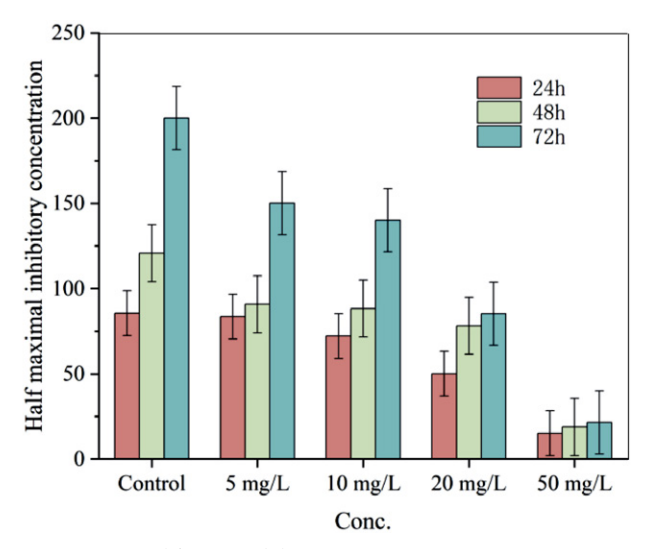
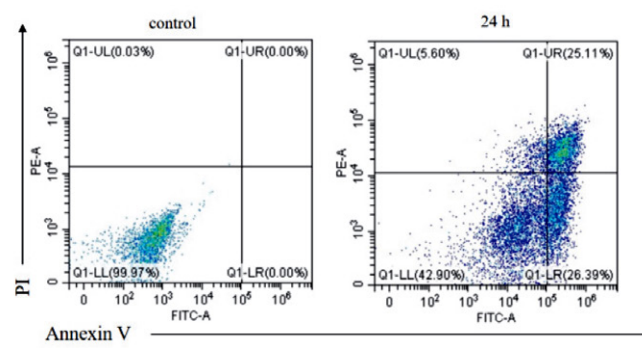
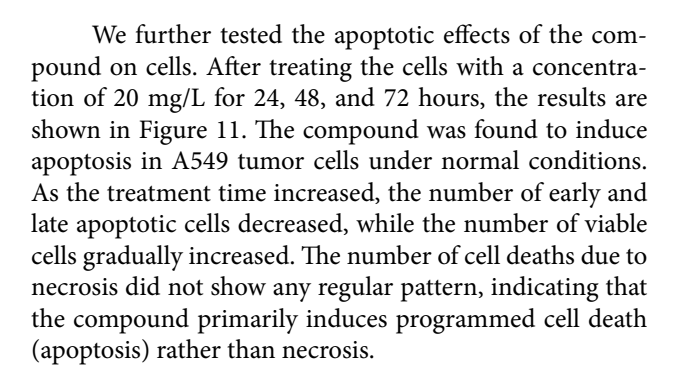


Figure 10. Proliferation inhibition activity assay





#### 4. Conclusions

In this work, network pharmacology, bioinformatic analysis and molecular were used to explore the possible pathways by which CAZ-AVI inhibits pneumonia. The findings showed that CAZ-AVI targets several important proteins that are involved in the control of multi-target mechanisms. In addition to its known antibacterial effects, CAZ-AVI also has other potential non-antibacterial effects. By inhibiting or activating these target proteins, it may play a regulatory role in cell proliferation, apoptosis, signal transduction, and immune responses. Molecular docking results showed good binding affinity of bioactive ingredients, as well as good stability and compactness with the respective targets. Our experimental results further confirmed that the compound possesses activities in inhibiting cell proliferation and promoting apoptosis. With the potential targets and pathways of CAZ-AVI clearly delineated in this study, it indicates that the pharmacological effects of the drug may cover multiple levels. It can not only directly inhibit bacterial growth, but also exert more complex pharmacological effects by regulating the signaling pathways and protein functions within the host cells. In the future, we will conduct in-depth validation of these mechanisms of action through in vitro and in vivo experiments. Indepth research on the interaction network between CAZ-AVI and these target proteins will help us gain a more comprehensive understanding of the drug's mechanism of action in the body, thereby providing a solid theoretical basis for personalized medicine and precision medicine.

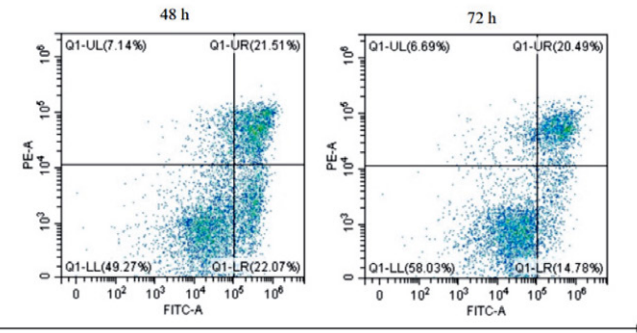


Figure 11. Annexin V-FITC/PI staining for apoptosis assay

#### Conflict of Interest

The authors declare no conflict of interest.

### 5. References

- 1. E. Montassier, G. D. Kitsios, J. E. Radder, Q. Le. Bastard, B. J. Kelly, A. Panzer, S. V. Lynch, C. S. Calfee, R. P. Dickson, A. Roquilly, *Nat. Med.* **2023**, *11*, 2793–2804.
  - DOI:10.1038/s41591-023-02617-9
- M. Miron, M. Blaj, A. I. Ristescu, G. Iosep, A. N. Avadanei,
   D. G. Iosep, R. Crisan-Dabija, A. Ciocan, M. Pertea, C. D. Manciuc, S. Luca, C. Grigorescu, M. C. Luca, *Microorganisms* 2024, 1,213. DOI:10.3390/microorganisms12010213
- A. Gauba, K. M. Rahman, Antibiotics (Basel) 2023, 12, 1590.
   DOI:10.3390/antibiotics12111590
- D. Hodyna, A. Klipkov, M. Kachaeva, Y. Shulha, I. Gerus,
   L. Metelytsia, V. Kovalishyn, *Chem. Biodivers.* 2024, 8, e202400638.
- M. Gatti, R. Pascale, P. G. Cojutti, M. Rinaldi, S. Ambretti, M. Conti, S. Tedeschi, M. Giannella, P. Viale, F. Pea, *Int. J. Antimicrob. Ag.* 2023, *1*, 106699.
  - DOI:10.1016/j.ijantimicag.2022.106699
- M. Gatti, M. Rinaldi, C. Bonazzetti, P. Gaibani, M. Giannella,
   P. Viale, F. Pea, Ann. Clin. Microbiol. Antimicrob. 2023, 11, e0096923.
- R. K. Shields, L. M. Abbo, R. Ackley, S. L. Aitken, B. Albrecht, A. Babiker, R. Burgoon, R. Cifuentes, K. C. Claeys, B. N. Curry, K. E. Desear, J. C. Gallagher, E. Y. Golnabi, A. E. Gross, J. Hand, E. L. Heil, K. M. Hornback, K. S. Kaye, T. V. Khuu, M. E. Klatt, E. G. Kline, R. C. Kubat, W. Kufel, J. H. Lee, A. J. Lepak, A. Lim, J. M. Ludwig, C. Macdougall, A. Majumdar, A. J. Mathers, E. K. Mccreary, W. R. Miller, M. L. Monogue, W. J. Moore, S. Olson, J. Oxer, J. C. Pearson, C. Pham, P. Pinargote, C. Polk, M. J. Satlin, S. W. Satola, S. N. Shah, P. Tamma, T. Tran, D. van. Duin, M. Vannatta, A. Vega, V. Venugopalan, M. P. Veve, W. Wangchinda, L. S. Witt, J. Y. Wu, J. M. Pogue, Lancet. Infect. Dis. 2025, 5, 574–584.
  - DOI:10.1016/S1473-3099(24)00648-0
- Y. X. Kang, J. C. Cui, Eur. J. Clin. Microbiol. 2025, 44, 1493– 1500. DOI:10.1007/s10096-025-05090-z
- R. Taha, O. Kader, S. Shawky, S. Rezk, Ann. Clin. Microb. Anti. 2023, 22, 21. DOI:10.1186/s12941-023-00578-y
- M. Hussein, R. Allobawi, J. X. Zhao, H. D. Yu, S. L. Neville, J. Wilksch, L. J. M. Wong, M. Baker, C. A. McDevitt, G. G. Rao, J. Li, T. Velkov, *Acs Infect. Dis.* 2023, 12, 2409–2422.
   DOI:10.1021/acsinfecdis.3c00264
- Z. H. Zheng, Z. Q. Shao, L. H. Lu, S. Y. Tang, K. Shi, F. X. Gong, J. Q. Liu, Sci. Adv. 2017, 8, e701102.
- 13. M. Shirley, *Drugs* **2018**, *6*, 675–692. **DOI:**10.1007/s40265-018-0902-x
- S. H. MacVane, J. L. Crandon, W. W. Nichols, D. P. Nicolau, *Ann. Clin. Microbiol. Antimicrob.* 2014, 11, 6913–6919.
   DOI:10.1128/AAC.03267-14
- Z. Y. Huang, Y. J. Han, X. T. Zhang, Y. Sun, Y. Z. Lin, L. Z. Feng, T. L. Zhou, Z. Y. Wang, *Bmc Microbiol.* 2023, 1, 321.

#### **DOI:**10.1038/s42004-024-01179-2

- Y. C. Chou, Y. H. Hsu, D. M. Lee, J. W. Yang, Y. H. Yu, E. C. Chan, S. J. Liu, Acs Biomater. Sci. Eng. 2024, 4, 2595–2606.
- 17. A. Daina, V. Zoete, Commun. Chem. 2024, 7, 105.
- K. Gallo, A. Goede, R. Preissner, B. O. Gohlke, *Nucleic Acids*. *Res.* 2022, *W1*, W726–W731. DOI:10.1093/nar/gkac297
- S. Fishilevich, R. Nudel, N. Rappaport, R. Hadar, I. Plaschkes, T. Iny. Stein, N. Rosen, A. Kohn, M. Twik, M. Safran, D. Lancet, D. Cohen, *Database* 2017, 2017, bax028.
  - DOI:10.1093/database/bax028
- N. Queralt-Rosinach, J. Piñero, À. Bravo, F. Sanz, L. I. Furlong, *Bioinformatics* 2016, 14, 2236–2238.
   DOI:10.1093/bioinformatics/btw214
- UniProt Consortium, Nucleic Acids. Res. 2021, D1, D480– D489
- 22. S. K. Burley, C. Bhikadiya, C. Bi, S. Bittrich, L. Chen, G. V. Crichlow, C. H. Christie, K. Dalenberg, L. Di. Costanzo, J. M. Duarte, S. Dutta, Z. Feng, S. Ganesan, D. S. Goodsell, S. Ghosh, R. K. Green, V. Guranović, D. Guzenko, B. P. Hudson, C. L. Lawson, Y. Liang, R. Lowe, H. Namkoong, E. Peisach, I. Persikova, C. Randle, A. Rose, Y. Rose, A. Sali, J. Segura, M. Sekharan, C. Shao, Y. P. Tao, M. Voigt, J. D. Westbrook, J. Y. Young, C. Zardecki, M. Zhuravleva, Nucleic Acids. Res. 2021, D1, D437–D451. DOI:10.1093/nar/gkaa1038
- C. S. Liu, J. P. Tong, Z. Y. Fang, X. M. Guo, T. T. Shi, S. R. Liu,
   J. Sun, Mol. Divers. 2025, DOI:10.1007/s11030-025-11111-y
- Z. J. Song, X. F. Wu, Z. Y. Zhou, J. J. Zhang, Y. Y. Pan, X. Dong, X. Pang, Y. P. Xie, J. Sun, Y. Zhang, J. Qin, *Eur. J. Med. Chem.* 2025, 286, 117286. DOI:10.1016/j.ejmech.2025.117286

# **Povzetek**

Ceftazidim-avibaktam (CAZ-AVI) je pokazal dobro učinkovitost pri zdravljenju pljučnice. Trenutno so raziskave o CAZ-AVI osredotočene predvsem na njegove neposredne protibakterijske učinke, medtem ko je raziskovanje njegovih možnih tarč v gostitelju razmeroma omejeno. V luči tega naša študija inovativno uporablja raziskovalno strategijo, ki združuje mrežno farmakologijo in računalniško podprto načrtovanje zdravil za sistematično raziskovanje potencialnih gostiteljskih tarč CAZ-AVI. Identificirali smo 141 skupnih tarč pri s CAZ-AVI zdravljeni pljučnici, med ključnimi tarčami pa so receptor za epidermalni rastni dejavnik (EGFR), protoonkogen Src (SRC), signalni pretvornik in aktivator transkripcije 3 (STAT3), toplotni šok protein 90 alfa, družina A, član 1 (HSP90AA1), kaspaza 3 (CASP3) in podenota jedrnega faktorja kapa B 1 (NFKB1). Z zaviranjem ali aktivacijo teh ciljnih proteinov ima CAZ-AVI pomembno regulacijsko vlogo pri celični proliferaciji, apoptozi, signalnem prenosu in imunskih odzivih. Naši eksperimentalni rezultati so dodatno potrdili, da ima spojina učinke pri zaviranju celične proliferacije in spodbujanju apoptoze. CAZ-AVI lahko popravi celično disfunkcijo in optimizira imunske odzive, s čimer zagotavlja nove strategije in vpoglede za zdravljenje pljučnice.



Except when otherwise noted, articles in this journal are published under the terms and conditions of the Creative Commons Attribution 4.0 International License